



Universiteit
Leiden
The Netherlands

Endogenous polyamines reduce the toxicity of soluble A β peptide aggregates associated with Alzheimer's disease

Luo, J.; Mohammed, I.; Wärmländer, S.K.T.S.; Hiruma, Y.; Gräslund, A.; Abrahams, J.P.

Citation

Luo, J., Mohammed, I., Wärmländer, S. K. T. S., Hiruma, Y., Gräslund, A., & Abrahams, J. P. (2014). Endogenous polyamines reduce the toxicity of soluble A β peptide aggregates associated with Alzheimer's disease. *Biomacromolecules*, 15(6), 1985-1991. doi:10.1021/bm401874j

Version: Publisher's Version

License: [Licensed under Article 25fa Copyright Act/Law \(Amendment Taverne\)](#)

Downloaded from: <https://hdl.handle.net/1887/3620634>

Note: To cite this publication please use the final published version (if applicable).

Endogenous Polyamines Reduce the Toxicity of Soluble A β Peptide Aggregates Associated with Alzheimer's Disease

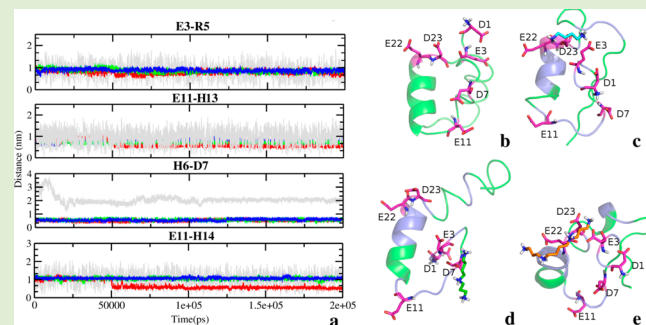
Jinghui Luo,[†] Inayathulla Mohammed,[†] Sebastian K. T. S. Wärmländer,[‡] Yoshitaka Hiruma,[†] Astrid Gräslund,[‡] and Jan Pieter Abrahams^{*†}

[†]Gorlaeus Laboratory, Leiden Institute of Chemistry, Leiden University, 2300RA Leiden, The Netherlands

[‡]Department of Biochemistry and Biophysics, Stockholm University, SE-10691 Stockholm, Sweden

S Supporting Information

ABSTRACT: Polyamines promote the formation of the A β peptide amyloid fibers that are a hallmark of Alzheimer's disease. Here we show that polyamines interact with nonaggregated A β peptides, thereby reducing the peptide's hydrophobic surface. We characterized the associated conformational change through NMR titrations and molecular dynamics simulations. We found that even low concentrations of spermine, spermidine, and putrescine fully protected SH-SY5Y (a neuronal cell model) against the most toxic conformational species of A β , even at an A β oligomer concentration that would otherwise kill half of the cells or even more. These observations lead us to conclude that polyamines interfere with the more toxic prefibrillar conformations and might protect cells by promoting the structural transition of A β toward its less toxic fibrillar state that we reported previously. Since polyamines are present in brain fluid at the concentrations where we observed all these effects, their activity needs to be taken into account in understanding the molecular processes related to the development of Alzheimer's disease.



INTRODUCTION

Amyloid aggregates, derived from amyloid protein fibrillation, are a hallmark of many neurodegenerative diseases, including Alzheimer's (AD), Parkinson's, and Huntington's diseases.¹ Oligomeric and fibrillar deposits of the A β peptide and the tau protein characterize Alzheimer's disease. The process of amyloid fibrillation has three different phases, lag, transition, and saturation, through which aggregating proteins first cluster into oligomers and then form fibrils. The early oligomers are especially toxic and the molecular background for their role as a driver of neurodegeneration has been investigated for many years.^{2,3} The mature amyloid fibrils can function as sources of secondary nucleation seeds for the more toxic oligomers, thereby regulating A β aggregation.⁴

There are many natural factors in neurons and in brain fluid that modulate the pathway of amyloid fibrillation, for example, the positively charged polyamines, which include spermine (SPN, +4), spermidine (SPD, +3), and putrescine (PUT, +2).^{5–7} Each of these polyamines have intracellular concentrations higher than 1 mM,⁸ and in cerebrospinal fluid, the total concentrations range between 0.4 and 0.8 μ M.⁹ Polyamines regulate important AD-related receptor–ligand interactions in neuronal cells.^{10,11} There are indications that brain polyamine levels are altered in AD patients.^{12,13} We recently reported that polyamines interact with the negatively charged residues of the A β peptide and significantly promote its fibrillation kinetics, as monitored by ThT and fluorescence spectroscopy.⁵ However,

the mechanism by which polyamines promote A β peptide fibrillation remains to be investigated, and their effect on the toxicity of A β peptide oligomers is still unknown. In the knowledge that the early aggregates of the A β peptide are the most toxic state and that the polyamines must bind to these early states in view of their pro-fibrillar activity, we investigated the effect of polyamines especially on the biophysical and functional (toxological) properties of these early aggregates.

Here we show that A β oligomers exhibit less hydrophobic surface in the presence of polyamines. Using a cell viability assay, we find that polyamines at (sub)physiological concentrations reduce the toxicity of A β oligomers. Although polyamines promote a structural transition of the A β peptide, we show that the structure of the nontoxic A β -polyamine oligomers retain a largely random coil structure in the lag phase. By NMR spectroscopy and *in silico* simulations, we explore the monomeric interaction between A β peptide and polyamines, leading to a model for binding that explains our NMR observations.

MATERIALS AND METHODS

Preparation of Monomeric and Oligomeric A β (1–40) Peptides. Monomeric A β : The 40 amino acid long amyloid- β

Received: December 19, 2013

Revised: April 17, 2014

Published: April 21, 2014

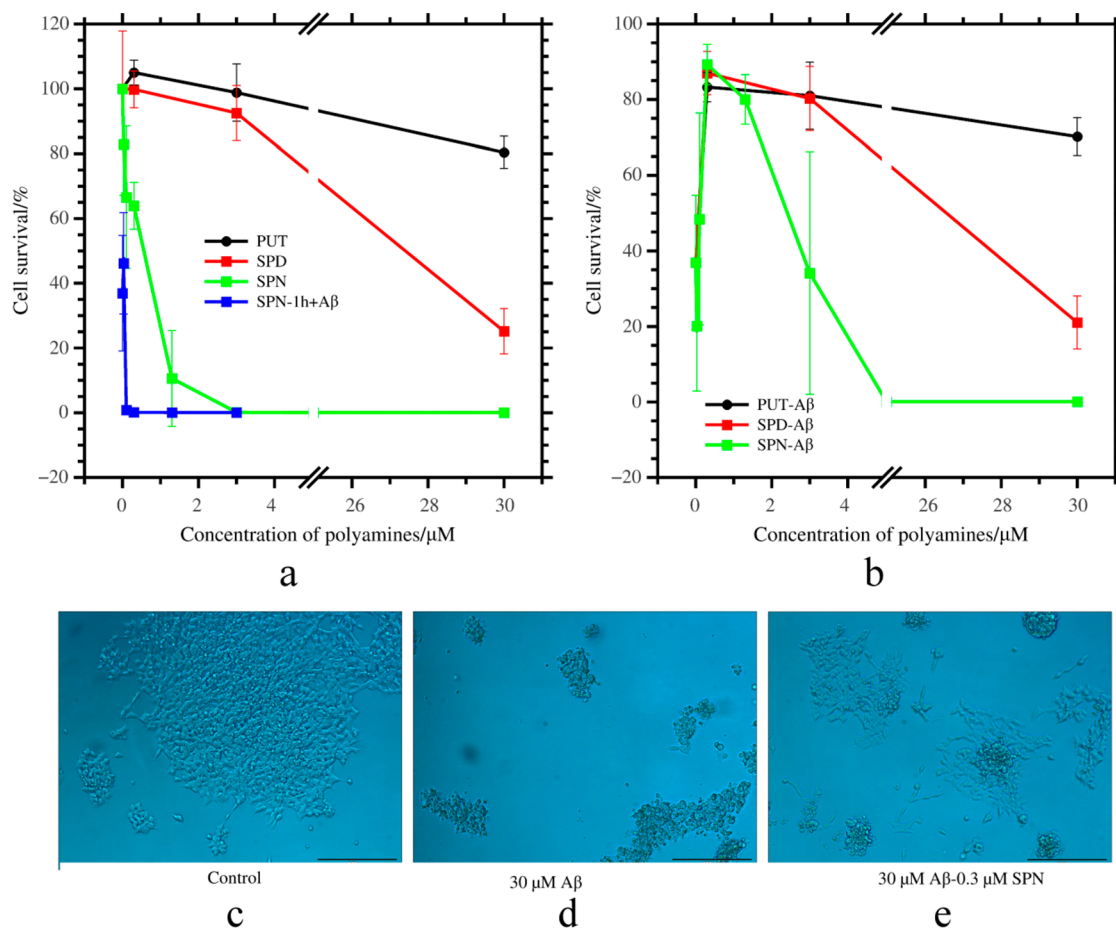


Figure 1. (a, b) Cell viability assay of SH-SY5Y cells after the incubation with polyamines (a), Aβ-polyamine oligomers (b), and Aβ oligomers (c), respectively. Shown as a blue curve in (a), free spermine was preincubated with neuronal cells for 1 h at different concentrations (0, 0.03, 0.1, 0.3, 1.3, and 3 μM) and then Aβ aggregates (obtained from peptide solutions that had been allowed to aggregate for 2 h at RT) were added to a final concentration of 30 μM (green curve). As a control, the black, red, and green curves in (a) indicate the percentage of surviving cells after incubation with free polyamines at the different concentrations of 0–30 μM. The black, red, and green curves in (b) display the cell survival rate after incubating with Aβ(30 μM) polyamine and Aβ(30 μM) oligomers. After incubating 100 μM Aβ with/without polyamines after 2 h preincubation at room temperature, we diluted these oligomers to final concentrations of 30 μM in experimental wells in the presence of 0, 0.03, 0.1, 0.3, 1.3, 3, 10, and 30 μM spermine and 0.3, 3, and 30 μM spermidine/putrescine, respectively. All of experiments were performed in triplicate to calculate the error bars and assuming controls in which only buffer, but neither Aβ, not polyamines were added, as representing 100% cell survival. The cell viability of neuronal cells was measured after 2 days incubation. (c, d) The cell morphologies after incubating with/without Aβ or Aβ-spermine oligomers for 2 days. The size of the bar is 250 μm.

peptide Aβ(1–40) was purchased from AlexoTech AB (Umeå, Sweden). The sample was dissolved to 2 mg/mL in 10 mM NaOH and sonicated for 1 min on ice according to previously described protocols. Then, Aβ(1–40) peptides in stock were diluted to appropriate concentrations.

Incubated Aβ: The Aβ peptides were diluted to 100 μM in PBS with 1 mM EDTA in the presence or absence of polyamines. Subsequently, the prepared samples were incubated for 2 h in Eppendorf tubes at room temperature and then used for different measurements. This procedure was prepared according to a published protocol.^{5,22}

1D NMR spectroscopy. A Bruker Avance 500 MHz spectrometer equipped with a triple-resonance cryogenically cooled probe head was used to record one-dimensional proton spectra at 5 °C of 68 μM Aβ(1–40) peptide in the presence and absence of polyamines in 20 mM sodium phosphate buffer at pH 7.3. TSP was used as a 0 ppm standard.

ANS Fluorescence Assay. Aliquots of the oligomeric Aβ were into a 384-well plate (optiplate 384, PerkinElmer), and 10 mM ANS was added. ANS fluorescence spectra between 400 and 600 nm were recorded with an Infinite M1000 PRO microplate reader, using excitation at 350 nm.

Cell Viability Assay. Neuroblastoma SH-SY5Y cells were used with a maximum passage number of 15. Cells were cultured in Dulbecco's modified eagle medium: a 1:1 mixture of DMEM and Ham's F12 medium and 10% supplemental fetal bovine serum, containing 1% (vol/vol) penicillin/streptomycin at 37 °C, 5% CO₂ in a 75 cm² flask (Greiner Bio-one, cat. 658170). In order to avoid using trypsin, cells were detached by 5 mM EDTA/PBS for 10 min in 37 °C. Then cells were resuspended at a concentration of 200000 cells/mL in DMEM/F12, containing 1% (vol/vol) penicillin/streptomycin. The resuspended cells were plated at a volume of 50 μL and a cell density of 20000 cells/well in a 96-well plate. The plated cells were incubated for 48 h at 37 °C at 5% CO₂. Aβ40 oligomer-enriched fractions were prepared at a concentration of 100 μM in the presence or absence of polyamines at room temperature for 2 h in PBS solution with 1 mM EDTA. The concentrations of the Aβ oligomers were diluted to final concentrations of 30 μM in experimental wells in the presence of 0, 0.03, 0.1, 0.3, 1.3, 3, 10, and 30 μM spermine and 0.3, 3, and 30 μM spermidine/putrescine, respectively. As a control, we incubated polyamines with neuronal cells at the different concentrations (0, 0.03, 0.1, 0.3, 1.3, 3, 10, and 30 μM spermine and 0.3, 3, and 30 μM spermidine/putrescine). To demonstrate the effects of free spermine on the Aβ neurotoxicity, we also first incubated free spermine with

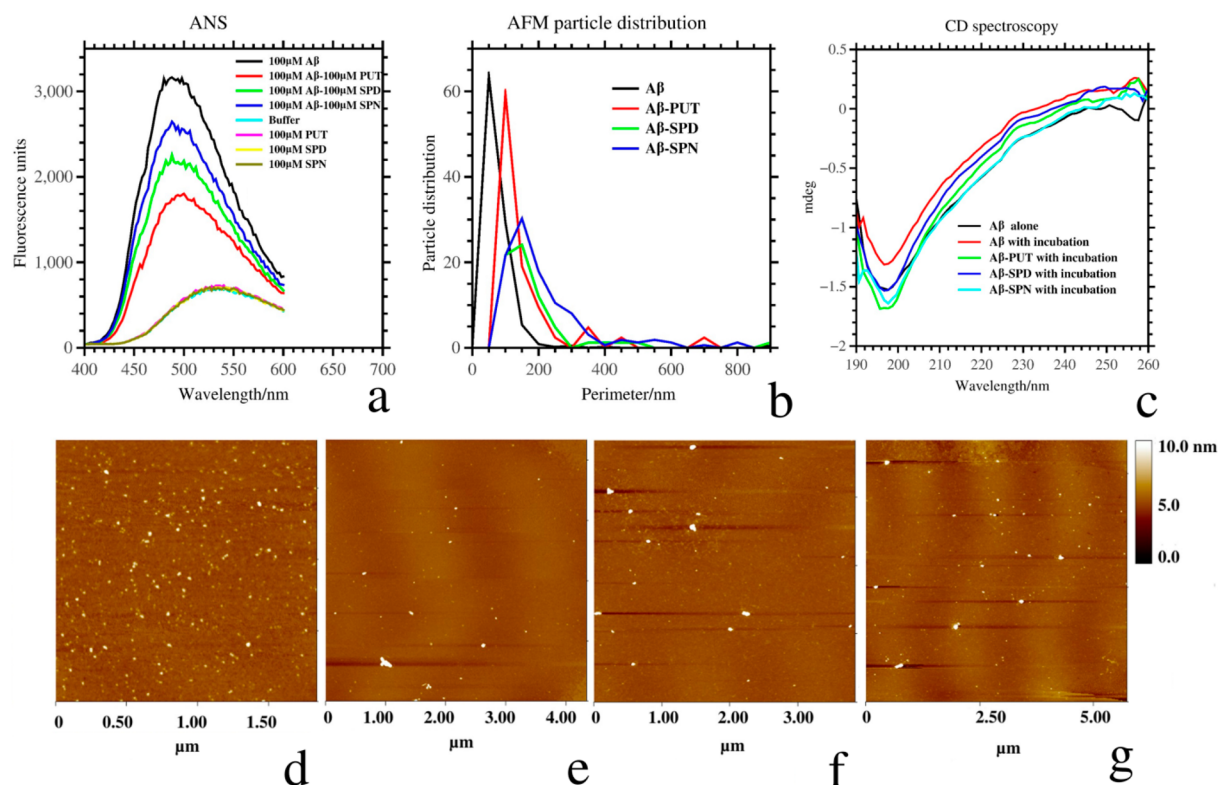


Figure 2. (a) ANS fluorescence spectroscopy of 100 μM $A\beta$ aggregates in the presence and absence of 100 μM polyamines after a 2 h incubation at room temperature. (b) The size distribution of the $A\beta$ aggregates calculated from AFM measurements. (c) CD spectroscopy of 5 μM $A\beta$ aggregates in the presence and absence of 5 μM polyamines. The samples were diluted from 2 h incubated, 100 μM $A\beta$ aggregates in the presence and absence of 100 μM polyamines at room temperature. As a control, $A\beta$ alone without incubation was also measured, shown as black curve. (e) AFM images of 100 μM $A\beta$ aggregates in the absence (d) and presence of 100 μM PUT (e), SPD (f), and SPN (g).

neuronal cells for 1 h at the different concentrations (0, 0.03, 0.1, 0.3, 1.3, and 3 μM) and then added $A\beta$ aggregates at the final concentration of 30 μM (same incubation procedure as above) to neuronal cells. The PBS control was added at a volume of 50 μL in medium to each well and left to incubate for 48 h. After 48 h, the plate was equilibrated at room temperature for approximately 30 min. CellTiter-Glo Luminescent (Promega, cat. G7571) compound was added to each well and then the contents in the plate were mixed on an orbital shaker for 2 min to induce cell lysis. This kit to measure the viability of SH-SY5Y cells^{14,15} and neurotoxicity of $A\beta$ aggregates^{16,17} has been applied to different studies. The ATP luciferase reaction that we used for the cell viability assay is shown in Figure S5. Luminescent intensity was measured on a 384-well plate reader (Infinite M1000 PRO microplate reader) at 1000 ms integration time. Measurements were performed in three independent experiments and statistical analysis was performed to calculate average values and standard deviations.

Isothermal Titration Calorimetry. Calorimetric measurements were performed on a VP-ITC (MicroCal). The sample cell contained 1 mL of 60 μM of $A\beta(1-40)$ peptide and the injection syringe 1 mM of spermine PBS buffer with 1 mM EDTA. Titration experiments were carried out at 298 K with 30 injections of 10 μL with 20 s duration and 350 s between each injection. The sample was mixed at 351 rpm.

Circular Dichroism (CD) Spectroscopy. CD spectroscopy was carried out on 400 μL samples of 5 μM $A\beta(1-40)$ peptide, diluted from 100 μM $A\beta(1-40)$ peptide after 2 h incubation, with or without polyamine (100 μM) in 5 mM sodium phosphate buffer at pH 7.3. The samples were put in a 1 mm path length quartz cuvette, kept at room temperature. CD spectra were recorded between 190 and 260 nm in a Chirascan CD unit from Applied Photophysics, Surrey, U.K.

Computational Protocol. A three-dimensional solution structure of the $A\beta(1-40)$ peptide in monomeric form, determined via solution NMR spectroscopy in the presence of SDS micelles,¹⁸ was

downloaded from the pdb database (www.rcsb.org/pdb, PDB entry 1BA4). The protonation states of the residues from $A\beta(1-40)$ peptide were predicted from H++ webserver (<http://biophysics.cs.vt.edu/>). Mol2 files of protonated spermine, spermidine, and putrescine were constructed from <http://nova.colombo58.unimi.it/moledit.htm>. Next, the polyamines were docked to the $A\beta$ -peptide with Autodock 4.119.¹⁹ The Lamarckian Genetic Algorithm was employed to search for energetically supported binding modes. The running number was 100, and 250000 energy evaluations were applied for each run. Autogrid box complexes between the three polyamines and the two $A\beta$ peptides were then built using AutoDockTools 1.4.6. The grid center was set in the center of the $A\beta$ peptide used, and the dimensions of the grid were 120 \times 120 \times 120 autogrid points with 0.375 \AA spacing. The atoms of the exocyclic group of the ligands were set as active torsions during docking. The evaluation of energy functions and free energies was run with analysis in tolerance of 2 \AA rmsd. Finally, the best docking conformations were selected via molecular dynamics simulations (below). MD simulations on polyamines together with the $A\beta(1-40)$ monomer were performed with the GROMACS version 4.5.1 suite of programs²⁰ using the Gromos force field. The parametrization of the force field for the inhibitor was performed via the PRODRG server.²¹ The $A\beta$ monomer structure was solvated in a cubic box of 12 \AA , cutoff with TIP3P water. Conjugated gradient algorithms were implemented for energy minimization with 1000 steps. In order to reduce close contact between the polyamines and the $A\beta$ peptides, the solvent system was heated to 300 K and equilibrated for 30 ps by a restraining simulation. During the unrestrained molecular dynamics simulation, the particle-mesh Ewald method was used to account for long-range electrostatic interactions. Temperature coupling and pressure coupling were conducted in the NpT ensemble, using a Berendsen thermostat of 300 K and 0.1 ps relaxation time, and a pressure of 0.5 bar with 0.000045 compressibility and 1 ps relaxation time. The LINCS algorithm was applied for all bond constraints. The MD simulations

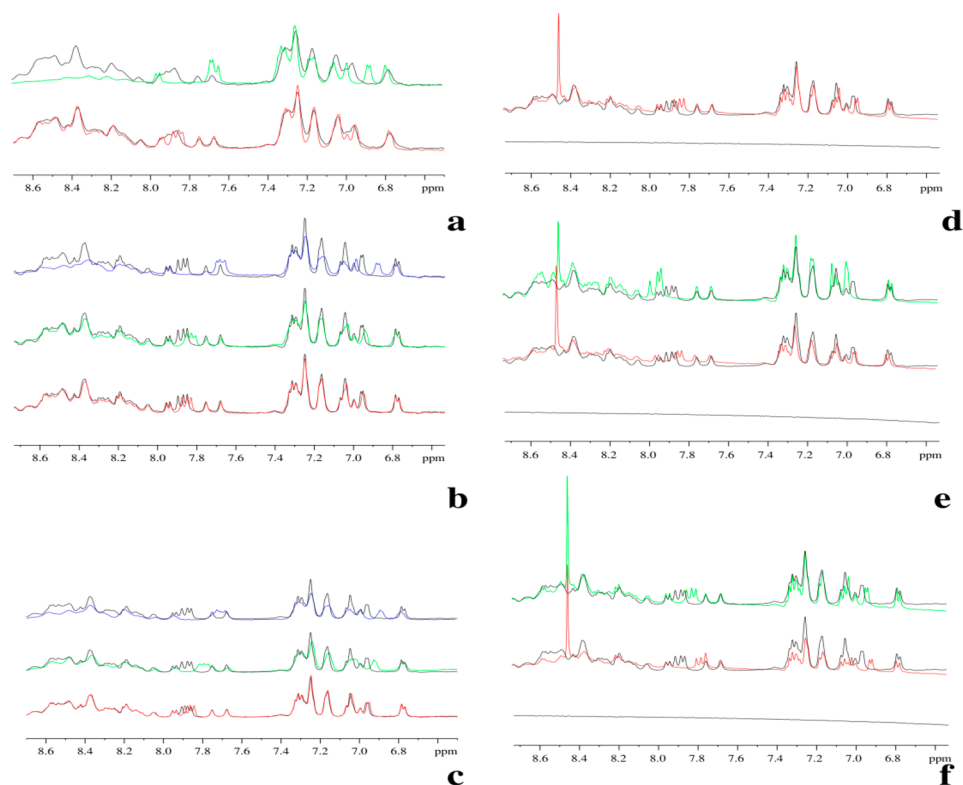


Figure 3. 1D proton NMR of $A\beta(40)$ peptide. (a–c) PUT (a), SPD (b), and SPN (c) were titrated into $68 \mu\text{M}$ $A\beta$ peptide (black line). The concentrations of PUT are $68 \mu\text{M}$ (red line) and $680 \mu\text{M}$ (green line) in (a). The concentrations of SPD are $68 \mu\text{M}$ (red line), $136 \mu\text{M}$ (green line), and $680 \mu\text{M}$ (blue line) in (b). The concentrations of SPN are $34 \mu\text{M}$ (red line), $68 \mu\text{M}$ (green line), and $272 \mu\text{M}$ (blue line) in (c). (d–f) $A\beta$ peptide were titrated into 0.15 mM PUT (d), SPD (e), and SPN (f) (the bottom black line), respectively. The concentrations of $A\beta$ are 0.05 mM (red line) in (d). The concentrations of $A\beta$ are 0.05 mM (red) and 0.15 mM (green line) in (e). The concentrations of $A\beta$ are 0.05 mM (red line) and 0.09 mM (green line) in (f). The superposed black line is $A\beta$ peptide alone spectroscopy. All of the figures are aligned by 1 mM trimethylsilyl propionate (TSP).³⁴

with 300 K were applied with 173529 seeds. As a control experiment, the $A\beta$ peptide monomer structure was simulated without polyamines using identical simulation methods. All resulting data were analyzed with GROMACS 4.5.1 subroutines including `g_rms`, `g_dist`, and `g_rmsf`, and `pymol` was employed to generate the molecular representations used in the study.

RESULTS

First, we confirmed by AFM and CD spectroscopy that significant $A\beta$ fibril formation had not started after incubating $100 \mu\text{M}$ monomeric $A\beta(1-40)$ peptide in the presence and absence of polyamines at room temperature for 2 h under nonagitating conditions, indicating the $A\beta$ peptides were still in the lag phase. Next, the toxicities of the $A\beta$ peptides after incubation with/without polyamines and free polyamines were measured in a cell viability assay using the SH-SY5Y neuronal cell model (Figure 1a,b). As shown in Figure 1a, survival of the neuronal cells decreased as we increased the concentration of free polyamine in the medium. Among the three different polyamines, spermine was the most toxic. After incubating with $30 \mu\text{M}$ $A\beta(1-40)$ aggregates, cell survival ranged between 10–50%. This is in line with earlier findings by others. For instance, using a Cell Titer-Blue Cell Viability Assay (Promega, cat. G8080) instead of the Cell-Titer-Glo assay we employed, Boersen et al. show that 90% of SH-SY5Y survived in $20 \mu\text{M}$ $A\beta(1-40)$ aggregates, whereas at $30 \mu\text{M}$ only 25% of the cells survived, suggesting an IC_{50} between 20 and $30 \mu\text{M}$.²² Since the aggregation of $A\beta$ peptide is a heterogeneous process, values measured in different experiments are expected to vary a bit.

Addition of polyamines in concentrations typically present in cerebrospinal fluid ($\sim 300 \text{ nM}$) during the $A\beta$ preincubation (preincubation is required to form the toxic, soluble $A\beta$ oligomers) reduced the toxicity of the $A\beta$ oligomers. It did not matter which polyamine we used: a similar protective effect was found for spermine, spermidine, and putrescine alike. At higher extracellular concentrations SPN and SPD turned out to be toxic to the SH-SY5Y cells, but these concentrations are not likely to be physiologically relevant. We observed that the cell survival rate sharply increased in the presence of low concentrations of spermine from 0.03 to $0.3 \mu\text{M}$. Therefore, the effects of spermine on the $A\beta$ associated neurotoxicity modulation are dose-dependency at the concentration of 0 – $0.3 \mu\text{M}$ spermine (green curve in Figure 1b). The polyamines might interact with certain kinases or receptors and increase the cell survival.^{23–25} To investigate the effects of free spermine on cell viability, we incubated free spermine at different concentrations with the cells for 1 h and then added $30 \mu\text{M}$ of $A\beta$ aggregates (or left the aggregates out as a control). Free spermine did not mitigate the neurotoxicity of $A\beta$ aggregates (Figure 1a (blue curve)), but spermine associated with the $A\beta$ aggregates did (Figure 1b (green curve)). Furthermore, observing cell morphologies (Figure 1c,d), we found that after adding the aggregates formed in the presence of $0.3 \mu\text{M}$ spermine and $30 \mu\text{M}$ $A\beta$, the cells retained similar morphologies as those observed in healthy cells. In contrast, most of the cells died in the presence of aggregates formed by $30 \mu\text{M}$ $A\beta$ without polyamines.

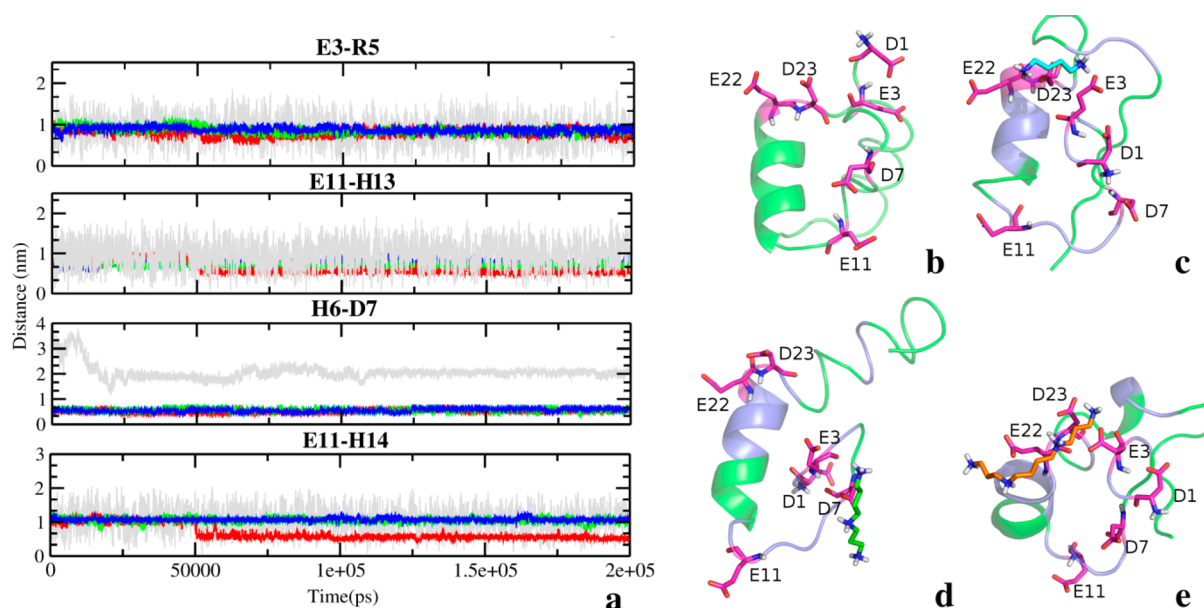


Figure 4. (a) The center distances of two charged residues in the N terminus of the peptide in the course of 200 ns MD simulations: gray, $A\beta$ alone; red, $A\beta$; and PUT: green, $A\beta$ and SPD; blue, $A\beta$ and SPN. (b–e) The snapshots before (a) and after 200 ns MD simulations of the $A\beta$ peptide in the absence (b) and presence of the polyamines putrescine (cyan sticks) (c), spermidine (green sticks) (d), and spermine (orange sticks) (e).

We investigated the binding affinity between spermine and $A\beta$ by calorimetry (Figure S1). The isotherm (Figure S1, upper panel) showed that the binding was exothermic. It also indicates a large negative enthalpy change (ΔH) and positive entropy (ΔS) at 298 K upon binding. Fitting the calorimetric curve using a one-site model yielded a dissociation constant of the 1:1 complex of about $25 \mu\text{M}$. However, a 1:1 complex may not be strictly appropriate, as the $A\beta$ peptide would be aggregating during the titration. Hence, the K_d of spermine bound to the $A\beta$ oligomer might be (substantially) lower than $25 \mu\text{M}$. In any case, this dissociation constant is low enough to indicate that during the preincubation of polyamine with $100 \mu\text{M}$ $A\beta$, most of the polyamine molecules were bound to $A\beta$.

Using the same sample, we characterized the effect of the polyamines on the surface hydrophobicity, secondary structure, and oligomeric state of the $A\beta$ peptide after the 2 h incubation. Using a 1-anilinonaphthalene-8-sulfonate (ANS) fluorescence assay,²⁶ we found that polyamines reduced the hydrophobic surface of the $A\beta$ -oligomers (Figures 2a and S2). SPN was the most active agent for modulating the hydrophobic surface of $A\beta$ oligomers. For measuring the effect of the polyamines on the secondary structure by CD spectroscopy, we diluted the concentration of the peptides from 100 to $5 \mu\text{M}$. We found that polyamines did not change the overall random coil nature of the $A\beta$ oligomers, but that some conformational changes were likely, as the polyamines reduced the CD signal for the $A\beta$ oligomers (Figure 2c). AFM indicated that $A\beta$ formed larger oligomers after 2 h incubation in the presence of polyamines (Figure 2b) compared to oligomers of $A\beta$ alone (Figures 2e,f and S3), and that fibrillation was not yet occurring. The reduction in hydrophobicity and the increase in size, both induced by the polyamines, might play a role in reducing the toxicity of the $A\beta$ aggregates.

In order to explore how polyamines might influence $A\beta$ oligomerization, we investigated the interaction between monomeric $A\beta$ and polyamines by 1D NMR and molecular modeling. First, polyamine was titrated into a solution of $A\beta$ peptide (Figure 3). Shifts of proton peaks (NH) induced by

polyamine were observed at Tyr10 (7.86) and at Ala2 (7.88) for all polyamines (all of peaks were assigned based on Table S1). At higher polyamine concentrations, Phe19 (HB/HG) shifted and, subsequently, all the other peaks either shifted or shrank. Then we titrated $A\beta$ into the polyamine solution, resulting in a similar pattern as was found in the first set of titration experiments, except that we also observed a single strong peak of unknown origin (8.46) in all cases. The extra peak might be caused by the presence trace amounts of formate (which has an NMR signal at 8.46), present in this particular batch of $A\beta$. The sharpness of the extra peak, compared to the signal of the peptide, indicates the molecule is not interacting with $A\beta$. Thus, polyamines interacted with $A\beta$ peptide by initially binding its N terminus, which is consistent with our previous study.³

We performed docking and molecular dynamic simulations to reveal the atomic details of the interaction between $A\beta$ peptide and polyamines (Figure 4). The α -helical starting structure of $A\beta$ was determined by solution NMR for $A\beta(1-40)$ bound to an SDS micelle.¹⁸ Although the α -helical starting structure of $A\beta$ does not agree with the random coil, observed by CD spectroscopy in solution, the peptide converts to random coil structure during simulation. After 200 ns molecular dynamic simulation, three polyamines were found to bind to the monomeric $A\beta$ peptide at slightly different sites. Spermidine interacted only with the $A\beta$ peptide N-terminus, forming hydrogen bonds with GLU3 and ASP7 (Figure 4e). Putrescine and spermine both interacted with $A\beta$ residues GLU3, GLU22, and ASP23, and spermine's longer carbon chain also had hydrophobic interactions with $A\beta$ residues 17–21(LVFFA) (Figure 4c–e).

As shown in Figure S4, $A\beta$ peptides with/without polyamines underwent secondary structural conversions throughout the 200 ns MD simulations. The initial α helix of the C-terminus (aa 31–40) disappeared in all cases after several nanoseconds. The transition from α -helix to β -sheet in the C-terminus of $A\beta$ peptide (i.e., aa 25–35) was more efficient in the presence of spermidine (after 15 ns). The C terminus of $A\beta$

peptides converted into a coil-bend-turn conformation after binding to spermine or putrescine. The N terminus of the $A\beta$ peptide, that is, highly charged residues D7-E11 converted into a random coil structure in the presence of polyamines but retained a bend structure in the absence of polyamines.

In order to investigate the effects of polyamines on the local structure of the $A\beta$ peptide, we analyzed the salt bridge network of $A\beta$ over the course of 200 ns. In the complexes of $A\beta$ -polyamine, the interaction between GLU3 and ARG5 remained stable, with a distance between residue centers of 0.75–1.2 nm during the simulation. In the absence of polyamines, this distance fluctuated between 0.25 and 1.75 nm. The distance between HIS6 and ASP7 remained stable (at 0.5 nm) in the presence of polyamines. In the absence of polyamines, this distance fluctuated between 2 and 4 nm in the beginning of 100 ns MD simulation, eventually reaching a stable distance of 2 nm. The distances between E11-H13 and E11-H14 of the $A\beta$ peptide remained constant at 0.75 nm in the presence of spermine or spermidine. With putrescine, the E11-to-H13 and E11-to-H14 distances were stable at 1 nm during the 50 first ns, and then dropped to a stable distance of 0.5 nm. In contrast, in $A\beta$ peptide alone, the E11-to-H13 and E11-to-H14 distances fluctuated frequently between 0.25 and 1.75 nm. We propose that the polyamine stabilized salt bridges in the $A\beta$ N-terminus. It is instructive to relate the interaction of $A\beta$ peptide-polyamines to other ligands such as apolipoprotein E (ApoE) and metal ions (Cu^{2+} and Zn^{2+}). ApoE4 promotes $A\beta$ peptide aggregation by frustrating the electrostatic network.²⁷ Cu(II)/Zn(II) interacts with N terminus of $A\beta$, thereby regulating the toxicity and fibrillation of $A\beta$.²⁸

DISCUSSION AND CONCLUSIONS

We have shown that $A\beta$ aggregates that formed in the lag phase in the absence of polyamines are smaller, more hydrophobic, and more toxic to neuronal cells, compared to similar aggregates formed in the presence of polyamines. Larger, less hydrophobic oligomers (containing polyamine) might not insert as readily into the cell membrane as the more hydrophobic and smaller $A\beta$ oligomers (without polyamine), or they might not be recognized as well by the RAGE receptors that are known to cross-react with $A\beta$ oligomers.²⁹ Furthermore, smaller oligomers would be expected to have a higher diffusion rate when inserted into the cellular membrane.³⁰ Also, it has been reported that the size of the hydrophobic surface of oligomeric aggregates positively correlates with toxicity to neural cells.²⁶

At the concentrations of $A\beta$ (100 μM) and polyamine (1 to 100 μM) used during the preincubations, most of the polyamines should have been in a 1:1 complex with $A\beta$ peptide, given the upper bound of the dissociation constant we measured (25 μM). Hence, the monomeric interaction between $A\beta$ and polyamine is important for understanding the effect of polyamines on the aggregation process of $A\beta$.

Our NMR experiments confirmed the monomeric interaction between polyamines and $A\beta$ and that the N-terminus of $A\beta$ is the most prominent interaction site. In silico simulations confirmed this observation as they indicated that polyamines stabilized the electrostatic network of the N terminus in $A\beta$ and thus perturb the conformational transition of $A\beta$ required for fibrillation. Hence, the polyamine- $A\beta$ oligomer may be packed somewhat differently. This would also explain why we observed that there is less hydrophobic surface on $A\beta$ -polyamine

oligomer by ANS fluorescence and why $A\beta$ -polyamine oligomers are larger than pure $A\beta$ oligomers.

Several types of amyloid oligomers can form during the lag phase. Small toxic prefibrillar oligomers (PFOs) require a conformational change before nucleating fibrils. It has been proposed that these PFOs interact with membrane lipids and induce the leakage of cells.³⁰ Nontoxic fibrillar oligomers (FOs) do not need such a conformational change in order to grow into mature fibrils.^{30,31} If we assume that polyamines promote the formation of FOs at the expense of the formation of PFOs, this would explain the reduction in toxicity and the promotion of $A\beta$ fibrillation by polyamines that we reported earlier.⁵ In another hypothesis of amyloid aggregate cytotoxicity, the cellular perturbation was proposed to be induced by the interaction of $A\beta$ with the RAGE receptor,²⁹ leading to oxidative stress. When $A\beta$ binds the RAGE receptor, this gives rise to an inflammatory response.³² Spermine inhibits this process by the down-regulating HMGB1 release, which, for instance, protects mice against Lethal Sepsis.³³ Spermine might also suppress the activity of RAGE and protect the neuronal cells. This hypothesis does not explain however, how spermidine and putrescine protect cells.

In conclusion, we have found that polyamines promote $A\beta$ fibrillation but reduce the toxicity of $A\beta$ oligomers. On the other hand, mature amyloid fibrils might be sources of secondary nucleation seeds for the more toxic oligomers. Perhaps polyamines can balance the toxicity of $A\beta$ oligomers and production of $A\beta$ fibrils. This mechanism of polyamines in $A\beta$ aggregation implicates that polyamines might play an important role in the regulation of $A\beta$ metabolism and even the development of AD disease. Levels of polyamines in brain fluids could be potentially used as a marker of the pathology of Alzheimer's disease.

ASSOCIATED CONTENT

Supporting Information

ANS spectroscopy (Figure S2) and AFM measurements (Figure S3) in polyamine/ $A\beta$ ratio of 0.01 and 0.1, and the secondary structure (Figure S4) in the course of 200 ns molecular dynamic simulations, the ATP luciferase reaction, and ITC measurements (Figure S1). This material is available free of charge via the Internet at <http://pubs.acs.org>.

AUTHOR INFORMATION

Corresponding Author

*E-mail: abrahams@chem.leidenuniv.nl

Notes

The authors declare no competing financial interest.

REFERENCES

- (1) Ross, C.; Poirier, M. *Nat. Med.* **2004**, *10 Suppl*, S11–7.
- (2) Rose, F.; Hodak, M.; Bernholc, J. *Sci. Rep.* **2011**, *1*, 1–5.
- (3) Benilova, I.; Karran, E.; De Strooper, B. *Nat. Neurosci.* **2012**, *15*, 349–357.
- (4) Cohen, S. I.; Linse, S.; Luheshi, L. M.; Hellstrand, E.; White, D. A.; Rajah, L.; Otzen, D. E.; Vendruscolo, M.; Dobson, C. M.; Knowles, T. P. J. *Proc. Natl. Acad. Sci. U.S.A.* **2013**, *110*, 9758–9763.
- (5) Luo, J.; Yu, C.-H.; Yu, H.; Borstnar, R.; Kamerlin, S. C. L.; Gräslund, A.; Abrahams, J. P.; Wärmländer, S. K. T. S. *ACS Chem. Neurosci.* **2013**, *4*, 454–462.
- (6) Fernández, C. O.; Hoyer, W.; Zweckstetter, M.; Jares-Erijman, E. a.; Subramaniam, V.; Griesinger, C.; Jovin, T. M. *EMBO J.* **2004**, *23*, 2039–2046.

- (7) Antony, T.; Hoyer, W.; Cherny, D.; Heim, G.; Jovin, T. M.; Subramaniam, V. *J. Biol. Chem.* **2003**, *278*, 3235–3240.
- (8) Casero, R. A.; Marton, L. J. *Nat. Rev. Drug Discovery* **2007**, *6*, 373–390.
- (9) Ekegren, T.; Gomes-Trolin, C. *Anal. Biochem.* **2005**, *338*, 179–185.
- (10) Soto, D.; Coombs, I. D.; Kelly, L.; Farrant, M.; Cull-Candy, S. G. *Nat. Neurosci.* **2007**, *10*, 1260–1267.
- (11) Berger, M. L.; Pöhler, T.; Schadt, O.; Stanger, M.; Rebernik, P.; Scholze, P.; Noe, C. R. *ChemMedChem* **2013**, *8*, 82–94.
- (12) Seidl, R.; Beninati, S.; Cairns, N.; Singewald, N.; Risser, D.; Bavan, H.; Nemethova, M.; Lubec, G. *Neurosci. Lett.* **1996**, *206*, 193–195.
- (13) Vivó, M.; de Vera, N.; Cortés, R.; Mengod, G.; Camón, L.; Martínez, E. *Neurosci. Lett.* **2001**, *304*, 107–111.
- (14) Dmitriev, R. I.; Ropiak, H. M.; Yashunsky, D. V.; Ponomarev, G. V.; Zhdanov, A. V.; Papkovsky, D. B. *FEBS J.* **2010**, *277*, 4651–4661.
- (15) Zhang, L.; Liu, W.; Szumlinski, K. K.; Lew, J. *Proc. Natl. Acad. Sci. U.S.A.* **2012**, *109*, 20041–20046.
- (16) Stine, W. B.; Jungbauer, L.; Yu, C.; Ladu, M. J. *Methods Mol. Biol.* **2011**, *670*, 13–32.
- (17) Jung, C.-G.; Uhm, K.-O.; Miura, Y.; Hosono, T.; Horike, H.; Khanna, K. K.; Kim, M.-J.; Michikawa, M. *Mol. Neurodegener.* **2011**, *6*, 47.
- (18) Coles, M.; Bicknell, W.; Watson, A. A.; Fairlie, D. P.; Craik, D. J. *Biochemistry* **1998**, *37*, 11064–11077.
- (19) Morris, G. M.; Huey, R.; Lindstrom, W.; Sanner, M. F.; Belew, R. K.; Goodsell, D. S.; Olson, A. J. *J. Comput. Chem.* **2009**, *30*, 2785–2791.
- (20) Hess, B.; Kutzner, C.; van der Spoel, D.; Lindahl, E. *J. Chem. Theory Comput.* **2008**, *4*, 435–447.
- (21) Schüttelkopf, A. W.; van Aalten, D. M. F. *Acta Crystallogr., Sect. D: Biol. Crystallogr.* **2004**, *60*, 1355–1363.
- (22) Broersen, K.; Jonckheere, W.; Rozenski, J.; Vandersteen, A.; Pauwels, K.; Pastore, A.; Rousseau, F.; Schymkowitz, J. *Protein Eng. Des. Sel.* **2011**, *24*, 743–750.
- (23) Kucharczywska, P.; Welch, J. E.; Svensson, K. J.; Belting, M. *Biochem. Biophys. Res. Commun.* **2009**, *380*, 413–418.
- (24) Eisenberg, T.; Knauer, H.; Schauer, A.; Büttner, S.; Ruckenstein, C.; Carmona-Gutierrez, D.; Ring, J.; Schroeder, S.; Magnes, C.; Antonacci, L.; Fussi, H.; Deszcz, L.; Hartl, R.; Schraml, E.; Criollo, A.; Megalou, E.; Weiskopf, D.; Laun, P.; Heeren, G.; Breitenbach, M.; Grubeck-Loebenstein, B.; Herker, E.; Fahrenkrog, B.; Fröhlich, K.-U.; Sinner, F.; Tavernarakis, N.; Minois, N.; Kroemer, G.; Madeo, F. *Nat. Cell Biol.* **2009**, *11*, 1305–1314.
- (25) Terui, Y.; Akiyama, M.; Sakamoto, A.; Tomitori, H.; Yamamoto, K.; Ishihama, A.; Igarashi, K.; Kashiwagi, K. *Int. J. Biochem. Cell Biol.* **2012**, *44*, 412–422.
- (26) Bolognesi, B.; Kumita, J. R.; Barros, T. P.; Esbjorner, E. K.; Luheshi, L. M.; Crowther, D. C.; Wilson, M. R.; Dobson, C. M.; Favrin, G.; Yerbury, J. J. *ACS Chem. Biol.* **2010**, *5*, 735–740.
- (27) Luo, J.; Maréchal, J.-D.; Wärmländer, S.; Gräslund, A.; Perálvarez-Marín, A. *PLoS Comput. Biol.* **2010**, *6*, e1000663.
- (28) Ghalebani, L.; Wahlström, A.; Danielsson, J.; Wärmländer, S. K. T. S.; Gräslund, A. *Biochem. Biophys. Res. Commun.* **2012**, *421*, 554–560.
- (29) Yan, S. D.; Zhu, H.; Zhu, A.; Golabek, A.; Du, H.; Roher, A.; Yu, J.; Soto, C.; Schmidt, A. M.; Stern, D.; Kindy, M. *Nat. Med.* **2000**, *6*, 643–651.
- (30) Glabe, C. G. *J. Biol. Chem.* **2008**, *283*, 29639–29643.
- (31) Laganowsky, A.; Liu, C.; Sawaya, M. R.; Whitelegge, J. P.; Park, J.; Zhao, M.; Pensalfini, A.; Soriaga, A. B.; Landau, M.; Teng, P. K.; Cascio, D.; Glabe, C.; Eisenberg, D. *Science* **2012**, *335*, 1228–1231.
- (32) Creagh-Brown, B. C.; Quinlan, G. J.; Evans, T. W.; Burke-Gaffney, A. *Intensive Care Med.* **2010**, *36*, 1644–1656.
- (33) Zhu, S.; Ashok, M.; Li, J.; Li, W.; Yang, H.; Wang, P.; Tracey, K. J.; Sama, A. E.; Wang, H. *Mol. Med.* **2009**, *15*, 275–282.
- (34) Maniara, G.; Rajamoorthi, K.; Rajan, S.; Stockton, G. W. *Anal. Chem.* **1998**, *70*, 4921–4928.